Electronic Supplementary Material

High Performance *In Vivo* Near-IR (>1 μm) Imaging and Photothermal Cancer Therapy with Carbon Nanotubes

Joshua T. Robinson[1], Kevin Welsher[1], Scott M. Tabakman[1], Sarah P. Sherlock[1], Hailiang Wang[1], Richard Luong[2], and Hongjie Dai[1] (✉)

[1] Department of Chemistry, Stanford University, Stanford, CA 94305, USA

[2] Department of Comparative Medicine, Stanford University School of Medicine, Stanford, CA 94305, USA

Supporting information to DOI 10.1007/s12274-010-0045-1

Table S-1 Serum chemistry and hematology data. We compared the blood chemistry of ten treated mice with control untreated mice 51 days post-injection and 48 days post-NIR laser irradiation at 0.6 W/cm^2 for 5 min. All values fall within the normal range for BALB/c mice (less than 1 year in age). Blood chemistry was also collected again for five treated mice 144 days post-SWNT injection. These data indicated that the liver, spleen, kidneys, and immune system were healthy and functioning. No toxic side affects were detected after injection of SWNTs. Blood was taken for analysis 51 days after injection of SWNTs and 48 days after NIR laser irradiation from all ten mice in the NIR irradiation + SWNT injection treatment group. Blood was also taken for analysis 163 days after injection of SWNTs and 160 days after NIR laser irradiation for five mice in the NIR irradiation + SWNT injected treatment group

Liver panel and blood chemistry	Units	Treated mice average (10 mice), day 51	Treated mice, day 51 (S. D.)	Treated mice average (5 mice), day 163	Treated mice, day 163 (S. D.)	Control mice average (5 mice), day 51	Control mice, day 51 (S. D.)	Reference ranges [S-1]
Aspartate aminotransferase	U/L	115.1	44.64	69	27.65	147.6	118.86	40–140
Alanine aminotransferase	U/L	83.9	13.37	35.2	13.59	80	30.64	30–100
Alkaline phosphatase	IU/L	111.1	18.36	83.8	40.03	193.8	62.82	47–275
Albumin	g/dL	2.27	0.61			2.56	0.55	1.3–2.6
Total protein	mg/dL	5.26	0.22			6.14	0.96	4.4–6.4
Phosphorus	mg/dL	4.66	1.65			7.2	1.09	4.5–8.9
Blood urea nitrogen	mg/dL	21.6	2.80			32.25	2.75	10–30
Cholesterol	mg/dL	73.1	7.09			80	20.19	N/A
Hematology								
White blood cell count	$\times 10^3/\mu L$	5.145	1.96	4.978	1.39	4.842	1.61	2.0–5.7
Red blood cell count	$\times 10^6/\mu L$	9.579	0.27	8.926	0.49	9.682	0.50	8.5–10.6
Hemoglobin	gm/dL	15.315	0.51	13.668	0.81	15.968	0.71	14.2–17
Hematocrit	%	44.72	1.17	40.48	2.18	44.97	3.08	38.3–47.9
Mean corpuscular volume	fL	46.64	0.60	45.38	0.31	46.64	0.71	40.9–50.3
Mean corpuscular hemoglobin	pg	16.01	0.46	15.32	0.28	16.56	0.46	15.1–18.4
Mean corpuscular hemoglobin concentration	g/dL	34.29	0.70	33.78	0.72	35.48	1.17	24.2–40.6

Address correspondence to hdai@stanford.edu

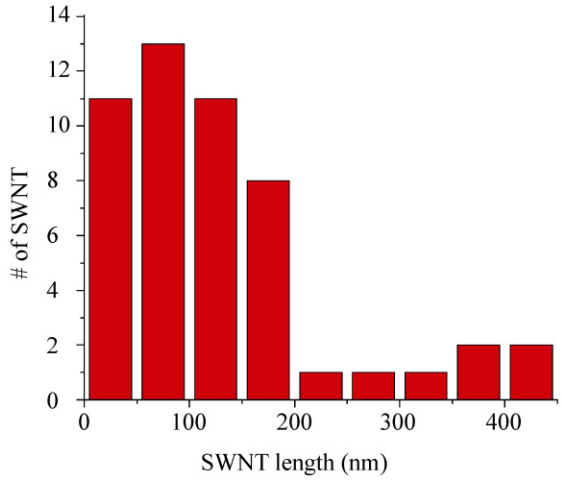

Figure S-1 AFM histogram of SWNT lengths. The lengths of the solubilized SWNTs were determined by AFM. The average length of 50 tubes was 137 nm

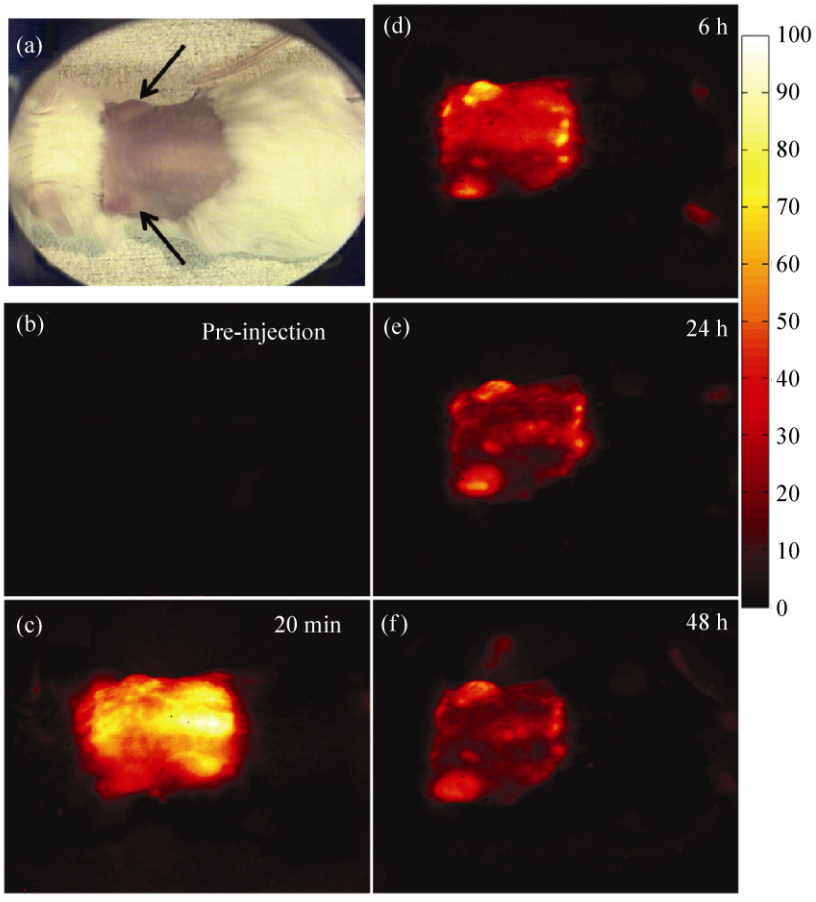

Figure S-2 *In vivo* NIR photoluminescence imaging of mice injected with SWNTs. (a) Optical image of a partially shaved BALB/c mouse with 4T1 tumors (indicated by arrows). NIR PL images were taken (b) pre-injection and at (c) 20 min, (d) 6 h, (e) 24 h and (f) 48 h post-injection. At early times, the NIR PL signal (1.1–1.4 μm) intrinsic to semiconducting SWNTs can be seen everywhere in the mouse as the SWNTs are circulating. At later times, high tumor contrast is seen due to the accumulation of SWNTs. Exposure time for all images is 300 ms

Table S-2 Photothermal efficiency of nanomaterials. A brief summary of the doses, NIR laser irradiation power, and effectiveness of various nanomaterials for photothermal tumor therapy

Material	Laser power (W/cm^2)	Irradiation time (min)	Injection dose (mg/kg)	Injection method[a]	Complete tumor destruction
SWNTs (*This work*)	0.6	5	3.6	i. v.	Yes
SWNTs [S-2]	1	5	1	i. s.	No
Gold nanorods [S-3]	2	5	20	i. v.	Yes
Gold nanorods (*This work*)	2	5	35	i. v.	Yes
Gold nanoshells [S-4]	4	3	N. A.[b]	i. v.	Yes
Indocyanine green [S-5]	52	3	50	i. s.	No
MWNTs [S-6]	2.5	1.16	1	i. s.	Yes
Gold nanocages [S-7]	0.7	10	50	i. v.	No

[a] Intravenous injection is abbreviated i. v.; Interstitial (Intra-tumor) injection is abbreviated i. s.

[b] Injection dose reported in terms of gold nanoshells/mL.

[S-1] Lee, J. H.; Sherlock, S. P.; Terashima, M.; Kosuge, H.; Suzuki, Y.; Goodwin, A.; Robinson, J.; Seo, W. S.; Liu, Z.; Lunong, R.; McConnell, M. V.; Nishimura, D. G.; Dai, H. J. High-contrast *in vivo* visualization of microvessels using novel FeCo/GC magnetic nanocrystals. *Magn. Reson. Med.* **2009**, *62*, 1497–1509.

[S-2] Zhou, F. F.; Xing, D.; Ou, Z. M.; Wu, B. Y.; Resasco, D. E.; Chen, W. R. Cancer photothermal therapy in the near-infrared region by using single-walled carbon nanotubes. *J. Biomed. Opt.* **2009**, *14*, 021009.

[S-3] von Maltzahn, G. Park, J. -H.; Agrawal, A.; Bandaru, K.; Das, S. K.; Sailor, M. J.; Bhatia, S. N. Computationally guided photothermal tumor therapy using long-circulating gold nanorod antennas. *Cancer Res.* **2009**, *69*, 3892–3900.

[S-4] O'Neal, D. P.; Hirsch, L. R.; Halas, N. J.; Payne, J. D.; West, J. L. Photo-thermal tumor ablation in mice using near infrared-absorbing nanoparticles. *Cancer Lett.* **2004**, *209*, 171–176.

[S-5] Chen, W. R.; Adams, R. L.; Higgins, A. K.; Bartels, K. E.; Nordquist, R. E. Photothermal effects on murine mammary tumors using indocyanine green and an 808-nm diode laser: an *in vivo* efficacy study. *Cancer Lett.* **1996**, *98*, 169–173.

[S-6] Ghosh, S.; Dutta, S.; Gomes, E.; Carroll, D.; D'Agostino, R.; Olson, J.; Guthold, M.; Gmeiner, W. H. Increased heating efficiency and selective thermal ablation of malignant tissue with DNA-encased multiwalled carbon nanotubes. *ACS Nano* **2009**, *3*, 2667–2673.

[S-7] Chen, J. Y.; Glaus, C.; Lafores, R.; Zhang, Q.; Yang, M. X.; Gudding, M.; Welch, M. J.; Xia, Y. N. Gold nanocages as photothermal transducers for cancer treatment. *Small* **2010**, *6*, 811–817.

[S-8] Prencipe, G. Tabakman, S. M.; Welsher, K.; Liu, Z.; Goodwin, A. P.; Zhang, L.; Henry, J.; Dai, H. J. PEG branched polymer for functionalization of nanomaterials with ultralong blood circulation. *J. Am. Chem. Soc.* **2009**, *131*, 4783–4787.

[S-9] Kam, N. W. S.; O'Connell, M.; Wisdom, J. A.; Dai, H. J. Carbon nanotubes as multifunctional biological transporters and near-infrared agents for selective cancer cell destruction. *Proc. Natl. Acad. Sci. USA* **2005**, *102*, 11600–11605.

[S-10] Nikoobakht, B.; El-Sayed, M. A. Preparation and growth mechanism of gold nanorods (NRs) using seed-mediated growth method. *Chem. Mater.* **2003**, *15*, 1957–1962.

[S-11] Liu, Z.; Davis, C.; Cai, W. B.; He, L. N.; Chen, X. Y.; Dai, H. J. Circulation and long-term fate of functionalized, biocompatible single-walled carbon nanotubes in mice probed by Raman spectroscopy. *Proc. Natl. Acad. Sci. USA* **2008**, *105*, 1410–1415.